

Temperature and Pressure Histories of End Gas under Knocking Condition in a S.I. Engine

E.Tomita, Y.Hamamoto and D.Jiang

*Department of Mechanical Engineering
Okayama University
3-1-1 Tsushima-naka, Okayama 700
Japan*

ABSTRACT

One of the methods for higher thermal efficiency of the internal combustion engine is limited due to knock, which is caused by autoignition of the unburned gas ahead of the flame. In order to understand the knock phenomena, it is important to measure the temperature of the unburned gas. In this study, a specially designed engine which could be ignited only once was used. The mixture was composed of n-butane, oxygen and argon. The temperature of the unburned end-gas was measured with a fiber optical interferometer system. When the density of the gas changes, the change of the optical path length of the test beam corresponds to the change of the refractive index. The temperature history of the unburned gas was determined by measuring the pressure and the change of the interference signal. As a result, it was confirmed that the laser interferometer system with polarization preserving fibers resisted the effect of mechanical vibration and that it was valid for investigating temperature history. Furthermore, the pressure and temperature histories of the unburned gas mixture were examined with an integral of the Livengood-Wu type.

INTRODUCTION

When a homogeneous gas mixture burns in a combustion chamber, pressure and the temperature of the unburned gas rise along with flame propagation. It is very important to know the temperature of the unburned end-gas when studies on burning velocity or ignition etc. are carried out. Moreover, because knock, which prevents a spark ignition engine from high efficiency, is caused by autoignition of an unburned mixture, it is necessary to know the temperature history of the unburned mixture in the end-gas region for investigating the condition of knock occurrence.

A sound velocity method and infrared emission-absorption method had been developed to apply to the measurement of unburned end-gas temperature ahead of the flame front at knock previously, and recently coherent anti-stokes Raman spectroscopy (CARS) is often used. Utilizing the fact that the sound velocity in a gas is proportional to the square root of the gas temperature, Livengood et al.[1]*

measured the temperature in an engine cylinder. Gluckstein and Walcutt[2] measured temperature histories of unburned end-gas under knock-limited compression ratio by using a few kinds of fuels with different octane numbers. Yamaga and Shibata[3] applied the frequency method, one kind of sound velocity method, to the measurement of gas temperature. The end-gas temperature was also measured with iodine absorption spectra by Chen et al.[4], a two-wavelength infrared method by Agnew[5], and infrared radiation pyrometer by Burrows et al.[6]. Lucht et al.[7] reviewed CARS for temperature measurement and measured the temperature of the unburned mixture with CARS under both knocking and non-knocking conditions. Otherwise, Nakada et al.[8]-[10] discussed the CARS measurements of unburned gas temperature in an engine combustion chamber in detail. Akihama et al.[11] improved the temperature resolution within $\pm 30\text{K}$ in the engine cylinder with CARS.

Laser interferometry has a high potential of resolution for temperature measurement. Garforth[12] and the authors[13] measured the temperature change of compressed unburned gas during the flame propagation by laser interferometry. It is very sensitive to mechanical vibration ordinarily. However, using this optical interference technique with some devices, it was confirmed that the history of unburned end-gas temperature could be measured just before the knock occurrence in the cylinder of a spark ignition engine[1-4]. In order to reduce the influence of mechanical vibration, a symmetrical Mach-Zehnder optical system involving polarization preserving fibers and Köster prisms was specially prepared. As a result, it was found that the temperature history of the unburned end-gas was measured just prior to knock occurrence. In this study, the temperature and pressure histories were compared under various conditions of spark timing, charging efficiency, equivalence ratio and engine speed. And the time at knock occurrence is discussed using the integral of Liengood-Wu type.

PRINCIPLE OF MEASUREMENT

Figure 1 shows the schematic diagram of the optical arrangement. A linear polarization beam for the measurement is provided by a He-Ne laser whose wavelength λ is $0.6328\ \mu\text{m}$ and the output is 15mW . The source beam is divided into two beams by a Koster prism after passing through a micro-

* Numbers in parentheses designate references at end of paper

lens and a polarization preserving fiber. While one beam passes through the outside of the combustion chamber as a reference one, another beam passes through the end-gas region of the combustion chamber as a test one as shown in Fig.1. Each beam passes through two glass rods in order to make the optical path as identical as possible. The two beams meet at another Köster prism and interfere with each other. With another optical fiber, the interfering light is guided to a phototransistor, and the intensity change of the interfering light is detected.

The density of unburned gas in the combustion chamber changes when it is compressed by a piston or flame propagation. Therefore the refractive index changes. Corresponding to the refractive index change in the end-gas region, the optical path difference between the test and reference beams varies, which causes the change of interference light intensity.

The change of optical path length, $\Delta\Phi$, has a relationship with number of intensity change, N .

$$\Delta\Phi = 2\pi N \tag{1}$$

When the refractive index of gas changes from the initial value, n_0 , to n , then the optical path difference change is given by

$$\Delta\Phi = 2\pi(n - n_0)L/\lambda, \tag{2}$$

where L denotes the thickness of the gas layer of the test section, and λ represents the wavelength of the He-Ne laser. The relationship between refractive index and density can be approximately expressed as

$$n = 1 + \rho R_G / M = 1 + PR_G / (MRT), \tag{3}$$

where R_G is Gladstone-Dale constant[15][m³/mole], which is determined by the wavelength of the laser and gas species; and

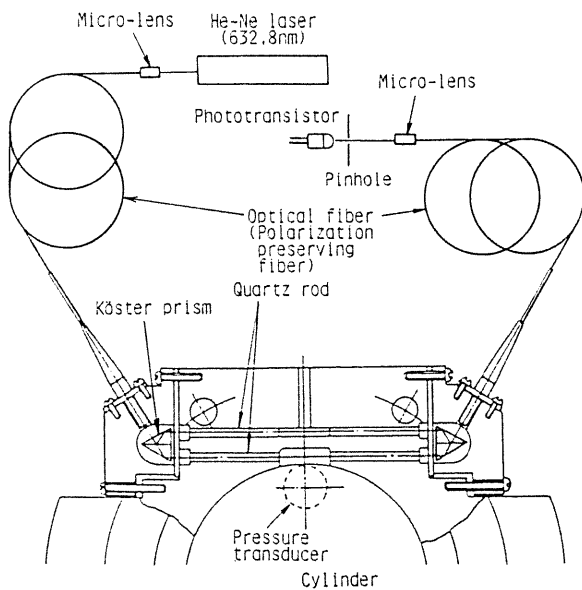


Fig.1 Test section in the combustion chamber and system of this optical interferometer.

M , R , P and T denote the mean molecular weight, the mean gas constant, pressure and temperature, respectively. The mean Gladstone-Dale constant may be calculated for a gas mixture containing a number of s species that contribute significantly to R_G from

$$R_G = \sum_{i=1}^s R_{Gi} x_i, \tag{4}$$

where x_i and R_{Gi} are respectively the mole fraction and the Gladstone-Dale constant of species i assuming that the mole fraction does not change from the initial state. The temperature of the unburned mixture can be given from Eqs. (1), (2) and (3).

$$T = LR_G T_0 P / (N \lambda M R T_0 + LR_G P_0) \tag{5}$$

When the pressure and temperature of initial state, P_0 and T_0 , respectively, are known, the temperature of the gas can be obtained by measuring the pressure and the number of the intensity change of the interfering light.

EXPERIMENTAL APPARATUS

In this experiment, a specially designed compression-expansion engine which could be ignited only once was used[16]. Figure 2 shows the schematic diagram of this engine. The engine had a bore and a stroke of 78 and 85mm, respectively. The compression ratio was 10.1. The engine cylinder was connected to a mixture tank through a pipe. At first, a homogeneous mixture was introduced in the tank and

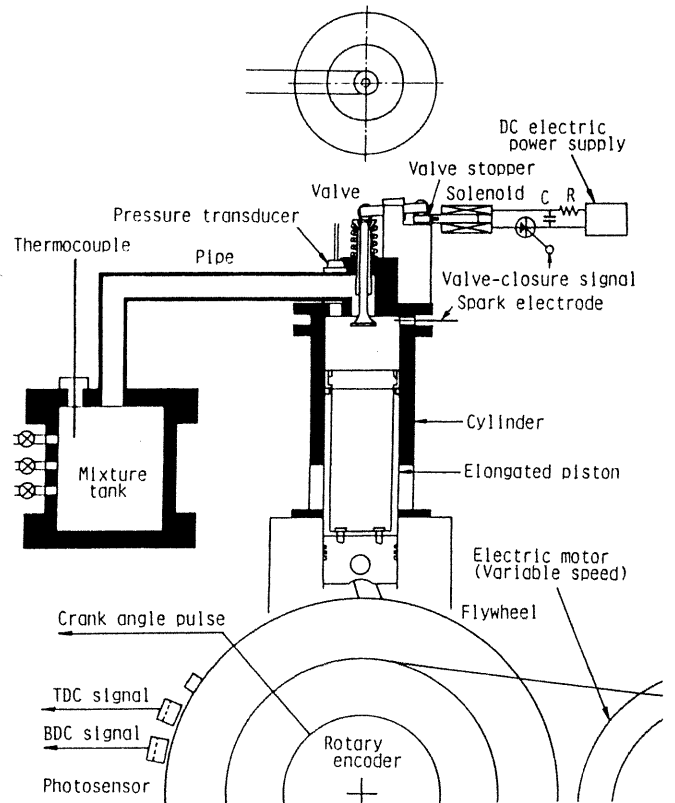
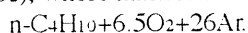


Fig.2 Schematic diagram of the specially designed single-event engine.

the cylinder under the conditions of opening the valve and setting the piston at a top dead center (TDC). The engine was driven by an electric motor while the valve was set in an open condition. After a given time, the valve was closed at a bottom dead center (BDC), and the gas was compressed and ignited by an electric spark at a selected crank angle to burn. The gas was introduced without swirl, because the valve was located at the center axis of the cylinder. Pressure in the cylinder, interference intensity, signals of crank angle, TDC, BDC and valve closure were recorded to the digital memory with a sampling time of 5 microseconds and data resolution of 12 bits. Normal-butane ($n\text{-C}_4\text{H}_{10}$) was used as a fuel and the composition of the homogeneous mixture was argon (Ar) and oxygen (O_2), whose mixture ratio were given as



As shown in Table 1, the experimental conditions are within engine speed, n , of 600~1200 rpm, equivalence ratio, ϕ , of 0.8~1.0, charging efficiency, η_c , of 0.36~0.48 and spark timing, θ_s , of 5~20° BTDC.

The gas condition at the beginning of compression which was taken as the base one had to be determined in advance, because only the change in temperature from the base state was measured by this laser interferometry. In this experiment, the valve was set to be closed at the BDC of the fifty-sixth cycle. Using a resistance wire as a thermometer, the temperature at the BDC at the valve closure cycle was measured. It was about 3.8K lower than the initial gas temperature in the mixture tank. According to this result, the temperature at the beginning of compression was determined.

The configuration of the test section of the engine combustion chamber is shown in Fig.1. The temperature of the unburned mixture at the test region which was at the opposite side of a pair of ignition electrodes was measured. The chamber has a height of 11.2 mm at TDC. The width of the gas layer at test region is 18.74 mm. The axis of the laser beam at the test region is 4.3 mm apart from the upper wall, and 2.7 mm from the side wall.

TEMPERATURE MEASUREMENT OF UNBURNED END-GAS IN ENGINE CYLINDER

Figure 3 shows the pressure and interference signal under the condition of $n=600\text{rpm}$, $\phi=1.0$, $\eta_c=0.48$ and $\theta_s=10^\circ$ BTDC. The bottom dead center corresponds to a crank angle of 180 deg., and the top dead center is 360 deg. The signals close to ignition are enlarged in Fig.4. The mixture was ignited at 10° BTDC, and then autoignition of end-gas occurred at about 3.5° ATDC to cause the knock. As shown in Fig.3, though the noise from the mechanical vibration got into the interference signal when the valve was closed at the bottom dead center, the influence was within the allowed range for measurement because the change of the signal was slower near the bottom dead center. It could be concluded from the signal shown in Fig.3 that the influence of the strike at the valve closing and engine operating vibration etc. was restrained sufficiently by using the symmetrical optical system shown in Fig.1. When the Köster prism as shown in Fig.1 was not used, the interference signal could not be read out owing to mechanical vibration. Figure 5 shows the number of the intensity change, N , presented in Fig.3 as the phototransistor signal. Both the bottom and top peaks of the

Table 1 Engine specifications and experimental conditions

Bore	78mm
Stroke	85mm
Compression ratio	10.1
Engine speed, n	600, 900 1200 rpm
Mixture	$n\text{-C}_4\text{H}_{10} + 6.5\text{O}_2 + 26\text{Ar}$
Equivalence ratio, ϕ	0.8, 0.9, 1.0
Charging efficiency, η_c	0.36~0.39, 0.41~0.43, 0.45~0.48
Spark ignition timing, θ_s	5, 10, 15, 20 °BTDC

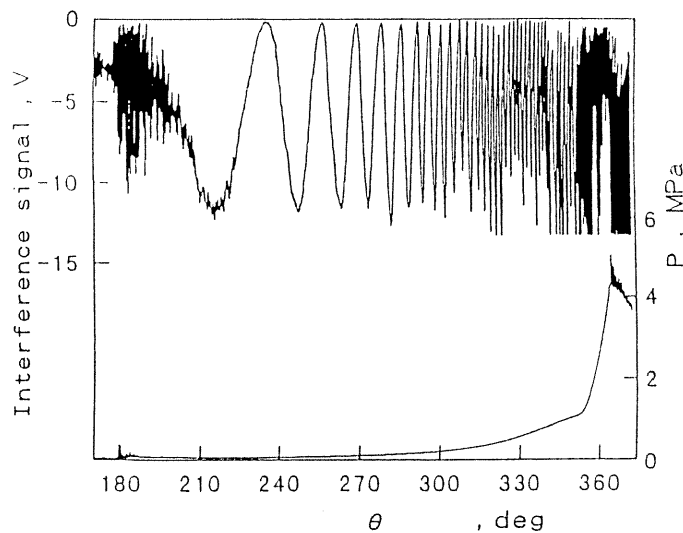


Fig.3 An example of interference signal and pressure in the cylinder of the single-event engine ($n=600$ rpm, $\theta_s=10^\circ$ BTDC, $\eta_c=0.48$).

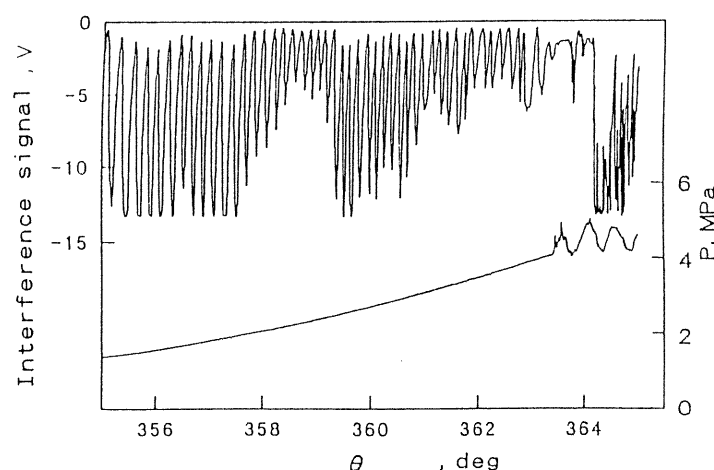


Fig.4 Interference signal and pressure in the cylinder, which are the same data in Fig.3 and enlarged near TDC.

signal could be read so that the resolution was $N/2$ in this study.

The temperature history of end-gas from the BDC to the time of knock occurrence was obtained from Eq.(5), with the number of the intensity change shown in Fig.5, the pressure in Figs.3 and 4 and the measured values of the initial state. Figure 6 and 7 are the results calculated in this way. The polytropic index from the bottom dead center to the spark

timing was calculated from the measured pressure and the volume of the cylinder. It was 1.445 from the bottom dead center to the crank angle of 270 deg. and 1.357 from 270 deg. to the spark timing. The gas temperature prior to spark ignition timing calculated by using these polytropic indices is shown with a dotted line in Fig.6. It is almost the same as the measured temperature by the interferometry. Assuming that the process of the gas change after the spark is adiabatic, the temperature history after spark was also calculated by using the measured pressure. The mean value of the ratio of specific heats within the temperature range of 650~1100K and pressure range of 1.0~4.0 MPa was 1.442. It was determined by considering the effect of temperature and pressure for argon and oxygen and that of temperature for normal-butane. The temperature on the assumption of adiabatic change was approximately equal to the measured one by the interferometry.

It is easy to distinguish the top and bottom peaks of interference signal. When we regard half a period of interference signal as the resolution of the interference signal, the measurement resolution of temperature, which changes

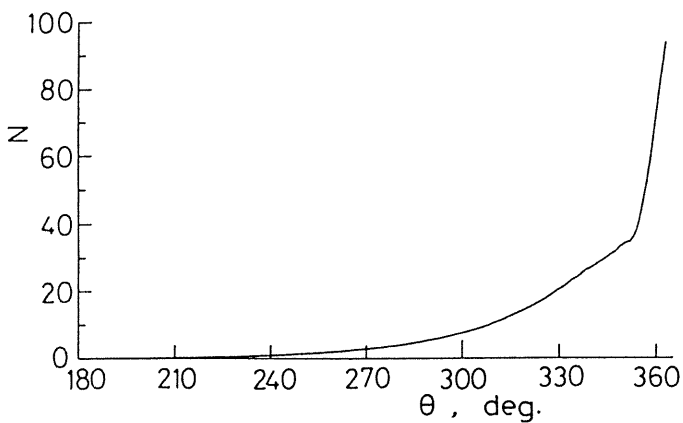


Fig.5 Number of change in interference intensity with phototransistor using the same data as in Fig.3.

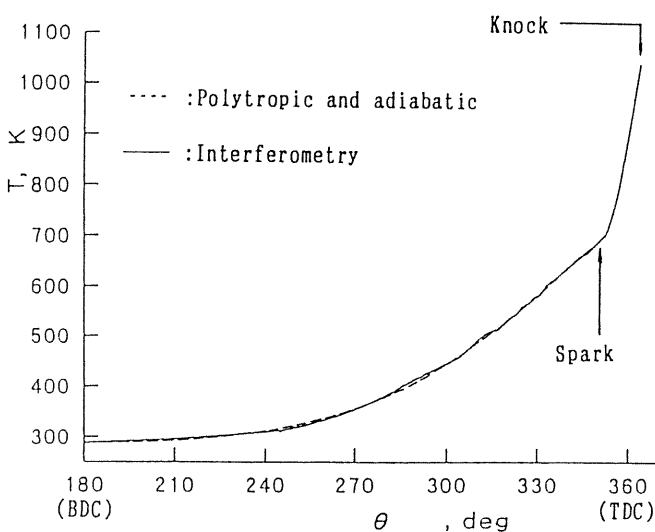


Fig.6 Temperature of unburned mixture in the cylinder determined from the data in Fig.3 ($n=600$ rpm, $\theta_s=10^\circ$ BTDC, $\eta_c=0.48$).

due to density, is about 5K just prior to the knock occurrence in this case. Of course, the interference signal could not be read sometimes due to the flame arrival to the test beam. In this study, such data was excluded.

HISTORIES OF PRESSURE AND TEMPERATURE OF UNBURNED END-GAS

Figure 8 shows examples of pressure and temperature histories of unburned end-gas in changing spark timing, θ_s , from 5 to 20°BTDC at $n=600$ rpm, $\phi=1.0$ and $\eta_c=0.45\sim 0.48$. The data of 10°BTDC in Fig.8 is different from the data in Figs.3~7. The measured temperature almost agreed with the value obtained on the assumption of polytropic and adiabatic change as described above.

Figure 9 shows the measured temperature of unburned end-gas at knock occurrence in changing spark timing at $n=600$ rpm, $\phi=1.0$ and $\eta_c=0.45\sim 0.48$. The black circle denotes the mean value of the temperature of the unburned end-gas at each same spark timing. The time from ignition to knock occurrence was almost the same even if the spark timing was changed.

The integral of Livengood-Wu type is used in prediction of the timing at knock occurrence[17]. The ignition delay time of the unburned mixture is defined as τ .

$$\int_0^{t_c} 1/\tau dt = K, \quad (6)$$

where 0 and t_c denote spark timing and prediction timing of knock occurrence, respectively, and the value of K would be unity. This integral is calculated along the change of pressure and temperature of the end-gas. The ignition delay of t is expressed as functions of pressure and temperature of unburned gas mixture.

$$\tau = A(P/P_0)^B \exp(C/T), \quad (7)$$

where P_0 denotes the standard pressure (=101.3 kPa), and B and C are empirical constants proposed by Roegenar[18], that is

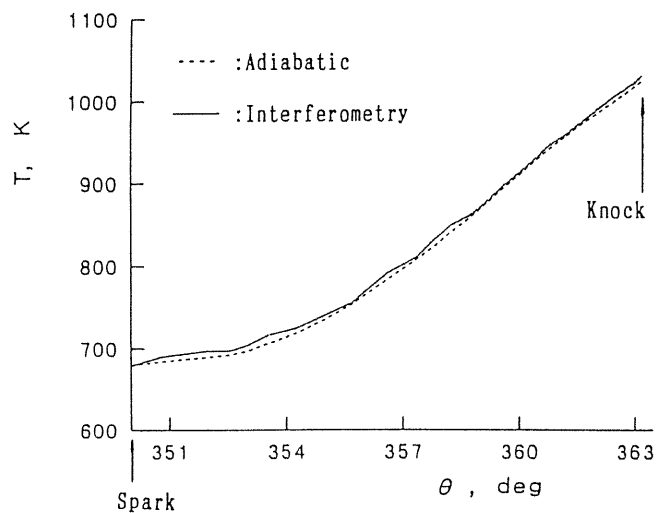
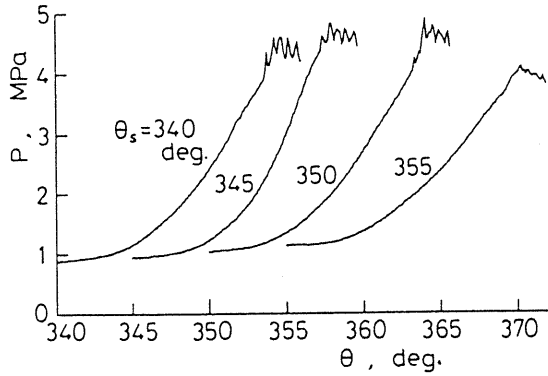
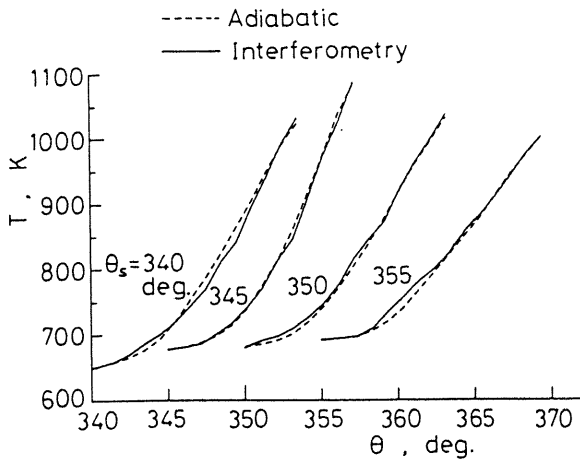


Fig.7 Temperature of unburned mixture in the cylinder determined from the data in Fig.3 near TDC.

to say, $B=-1.35$ and $C=8330$ [K]. A is also empirical constant, which is determined by satisfying the knock occurrence time of t_e for all experimental data as shown in Table 1 as well as possible. When 2.67×10^{-5} [s] was chosen as the value of A , the relationship between the value of t_e obtained in this way and the value of t_k from the experiment is presented in Fig. 10. However, all the data investigated here are not always



(a) Pressure history



(b) Temperature history

Fig.8 Histories of pressure and temperature of end-gas under the condition of various spark timing.

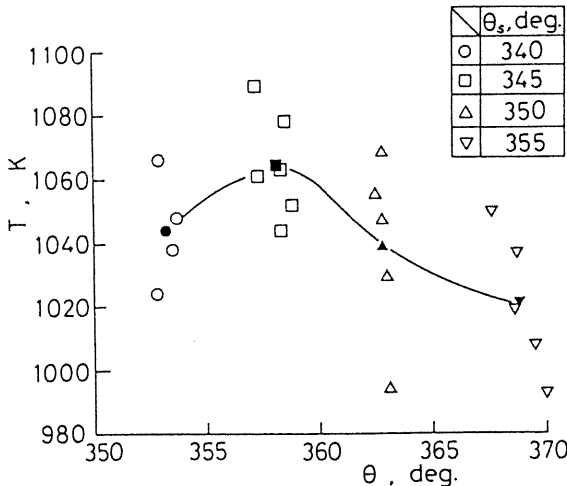


Fig.9 Temperature of end-gas at time of knocking occurrence under the condition of various spark timing.

shown in Fig.9 because the value of t_e can not be calculated for lack of pressure and temperature data in the case of $K < 1$ at the time of t_k .

As shown in Figure 11, the value of K was calculated from the temperature and pressure versus crank angle from the spark to the knock occurrence timing in changing spark timing at $n=600$ rpm, $\phi=1.0$ and $\eta_c=0.45-0.48$ as same data as in Fig.9. The value of K exceeded unity in some cases and did not reach unity in other cases. Figure 12 shows the distribution of the integral value, K , of Eq.(6) for all the data in changing equivalence ratio, engine speed, spark timing and

	θ_s ° BTDC	η_c	ϕ	n rpm
□	20	0.45 ~ 0.48	1.0	600
●	15	↑	↑	↑
○	10	↑	↑	↑
■	5	↑	↑	↑
◇	15	↑	↑	1200
▲	↑	0.41 ~ 0.43	↑	600
△	↑	0.36 ~ 0.39	↑	↑
▽	↑	0.45 ~ 0.48	0.9	↑
▼	↑	↑	0.8	↑

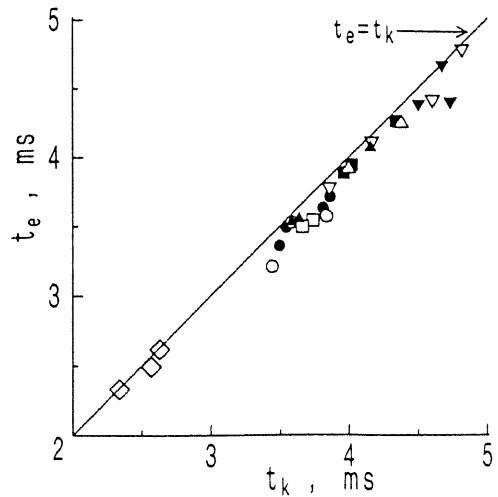


Fig.10 Relationship between predicted time of t_e and measured time of t_k .

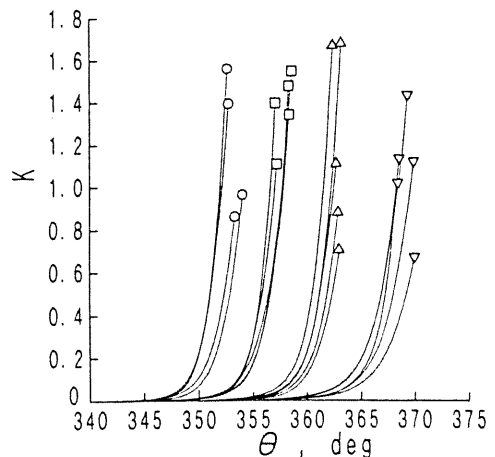


Fig.11 Value of Livengood-Wu integral, K

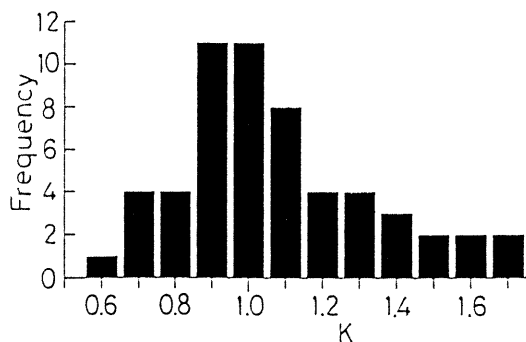


Fig.12 Distribution of value of Livengood-Wu integral, K

charging efficiency. The distribution of K seems to broaden widely. However, even if the value of K is changed in this way, the prediction time of t_e changes within about 0.2 ms because the value of the Livengood-Wu integral increases exponentially as shown in Fig.11.

CONCLUSIONS

The measurement method of gas temperature with this optical interferometry system has a high sensitivity by reducing mechanical vibration. The temperature history of unburned end-gas was measured from the beginning of compression to the knock occurrence by this laser interferometry in this study because the interference signal could be read clearly. And, it is confirmed that the temperature till spark timing changes polytropically and that the temperature from spark timing to knock occurrence is nearly equal to the value which is assumed with adiabatic change. Further, an integral of the Livengood-Wu type was adopted to discuss the temperature and pressure histories and the prediction of the timing of the knock occurrence. As a result, this integral is found to be approximately good under the conditions in this study.

REFERENCES

- [1] Livengood, J. C., Taylor, C. F. and Wu, P. C., "Measurement of Gas Temperature in an Engine by the Velocity of Sound Method", SAE Trans., Vol.66(1958), pp.683-699.
- [2] Gluckstein, M. E. and Walcutt, C., "End-gas Temperature-Pressure Histories and Their Relation to Knock", SAE Trans., Vol.69(1961), pp.529-553.
- [3] Yamaga, J. and Shibata, S., "Measurement Method of Gas Temperature by Using Ultra Sonic (4th Report, Temperature Measurement of Combustion Gas in Cylinder of Internal Combustion Engine)", Trans. of JSME, (in Japanese), Vol.36, No.286(1970), pp.1000-1005.
- [4] Chen, S. K., Beck, N. J., Uyehara, O. A. and Myers, P. S., "Compression and End-gas Temperature from Iodine Absorption Spectra", SAE Trans., Vol.62(1954), pp.503-513.
- [5] Agnew, W. G., "End Gas Temperature Measurement by a Two-Wavelength Infrared Radiation Method", SAE Trans., Vol.68(1960), pp.495-513.
- [6] Burrows, M. C., Shimizu, S., Myers, P. S. and Uyehara, O. A., "The Measurement of Unburned Gas Temperature in an Engine by an Infrared Radiation Pyrometer", SAE Trans., Vol.66(1961), pp.514-528.
- [7] Lucht, R. P., Teets, R. E., Green, R.M., Palmer, R.E. and Ferguson, C. R., "Unburned Gas Temperature in an Internal Combustion Engine. I: CARS Temperature Measurements", Combust. Sci. and Tech., Vol.55(1987), pp.41-61.
- [8] Nakada, T., Ito, T. and Takagi, Y., "Measurement of Unburned Gas Temperature Distribution by CARS on a Spark Ignition Engine under Knocking and Nonknocking Conditions", Trans. of JSAE (in Japanese), 24-2(1993), pp.10-14.
- [9] Nakada, T., Itoh, T. and Takagi, Y., "Unburnt Gas Temperature Measurements Using Single Shot CARS in a Spark Ignition Engine", Proc. of Symp. on COMODIA90, (1990), pp.393-399.
- [10] Nakada, T., Itoh, T. and Takagi, Y., "CARS Measurement of the Unburned Gas Temperature under Knocking and Non-knocking Operation and Residual Mass Fraction Variations in a Spark Ignition Engine", (in Japanese), The 10th Internal Combustion Engine Symposium in Japan (1992), pp.289-294.
- [11] Akihama, K., Asai, K., Kubo, S., Nakano, M., Yamazaki, S. and Iguchi, S., "Unburned Gas Temperature Measurements by CARS in a Spark-Ignition Engine", (in Japanese), The 10th Internal Combustion Engine Symposium in Japan(1992), pp.283-288.
- [12] Garforth, A. M., "Unburnt Gas Density Measurement in a Spherical Combustion Bomb by Infinite-fringe Laser Interferometry", Combust. Flame, Vol.26(1976), pp.343-352.
- [13] Hamamoto, Y., Tomita, E. and Okada, T., "The Measurement of the Transient Temperature of Gas by Laser Interferometry", JSME International Journal, Series II, Vol.32, No.2(1989), pp.247-251.
- [14] Hamamoto, Y., Tomita, E. and Jiang, D., "Temperature Measurement of End Gas under Knocking Condition in a Spark-Ignition Engine by Laser Interferometry", JSAE Review, 15-2(1994), to be published.
- [15] Gardiner, Jr. W.C., Hidaka, Y. and Tanzawa, T., "Refractivity of Combustion Gases", Combust. Flame, Vol.40(1981), pp.213-219.
- [16] Hamamoto, Y., Tomita, E., Tanaka, Y., Katayama, T. and Tamura, Y., "The Effect of Swirl on Spark-Ignition Engine Combustion", JSME International Journal, Vol.30, No.270 (1987), pp.1995-2002.
- [17] Livengood, J. C. and Wu, P. C., "Correlation of Autoignition Phenomena in Internal Combustion Engines and Rapid Compression Machine", 5th Symp. (Intern.) on Combust., (1955), pp.347-356.
- [18] Hatta, K., Asanuma, T. and Matsuki, M. eds., "Handbook of Internal Combustion Engine", (in Japanese), (1955), p.53, Asakura.